BULLETIN OF THE POLISH ACADEMY OF SCIENCES
TECHNICAL SCIENCES, Vol. 68, No. 5, 2020
DOI: 10.24425/bpasts.2020.134660

Stator winding fault diagnosis of induction motor operating under the field-oriented control with convolutional neural networks

M. SKOWRON, M. WOLKIEWICZ and G. TARCHAŁA*

Wrocław University of Science and Technology, Department of Electrical Machines, Drives and Measurements,
Wybrzeże Wyspiańskiego 27, 50-370 Wrocław, Poland

Abstract. In this paper deep neural networks are proposed to diagnose inter-turn short-circuits of induction motor stator windings operating under the Direct Field Oriented Control method. A convolutional neural network (CNN), trained with a Stochastic Gradient Descent with Momentum method is used. This kind of deep-trained neural network allows to significantly accelerate the diagnostic process compared to the traditional methods based on the Fast Fourier Transform as well as it does not require stationary operating conditions. To assess the effectiveness of the applied CNN-based detectors, the tests were carried out for variable load conditions and different values of the supply voltage frequency. Experimental results of the proposed induction motor fault detection system are presented and discussed.

Key words: diagnostics, stator faults, field-oriented control, convolutional neural networks.

1. Introduction

Induction motors (IM) are currently the most common group of electrical machines in the industrial systems. During the operation of these machines various types of damage can occur. Their causes may be due to both incorrect operation and manufacturing errors. About 38% of all IM defects, relate to stator [1]. They result from gradual degradation of the insulation, most often due to temperature changes, local displacement of the coils, as well as external conditions (dust, humidity) [2]. Electrical failures are characterized by high dynamics of the defect handling. Therefore, methods of early detection of coil short circuits become extremely important.

Currently used electrical machine diagnostic systems can be divided into systems using the analysis of diagnostic signals [3–5] and diagnostic techniques based on artificial intelligence [6, 7]. Among the analytical methods of detecting failures of the electrical machines the most common is the analysis of the diagnostic signal in the frequency domain (FFT – Fast Fourier Transform) [4]. It consists of the observation of the signal amplitudes emphasized in the spectrum at the frequencies characteristic for a given damage. Despite the widespread use of the FFT, this method has limitations that force a gradual departure from this technique of analysing the diagnostic signal. This is due to the need to ensure the stationarity of the diagnostic signals during the measurement, which in many cases is impossible to achieve. In addition, the efficiency of failure symptom extraction is strongly connected with the number of measured samples of the diagnostic signal (measurement time). In most cases, extraction of the damage symptoms from the diagnostic signals requires a few seconds measurement to maintain the appropriate FFT spectrum resolution. In the modern diagnostic systems, shortening the process time is a priority due to the nature of the defect, such as coil short circuits. This task requires full automation of the process, which is not ensured by known analytical methods. To reduce the role of experts and ensure full automation, artificial intelligence techniques are used in diagnostic processes.

Analytical methods are undoubtedly the basis for the development of neural defect detectors. Artificial intelligence techniques, and particularly artificial neural networks, are designed to evaluate the technical condition of a machine in accordance with the input information, which is most often the result of signal analysis. In the diagnostic systems, the most popular among the known neural structures are multi-layer perceptrons [8, 9], radial basis function neural networks [10], self-organizing Kohonen maps [11, 12] and wavelet neural networks [13]. These structures have a common feature, which is the need to provide initial processing of the diagnostic signals to identify the symptoms that constitute the input vector of a neural network. Classical neural structures were successfully used in the tasks of detection [13], classification [11] and the assessment of the degree of individual damage [9]. Ensuring automation of the process also proved the advantage of neural detectors over analytical methods of detection. However, the need to perform an initial analysis of the signal, and thus increase the detection time, requires further optimization of the diagnostic processes. The solution to the problem of preliminary processing of the diagnostic signal may be the Deep Neural Networks (DNNs). Deep neural structures are characterized by different features compared with classic neural networks, obtained by abandoning the rule of universal approximation.

In the last few years, only a few solutions using deep learning methods in diagnostic processes have been developed [14–22]. Most of the applications are related to mechanical

*e-mail: grzegorz.tarchala@pwr.edu.pl

Manuscript submitted 2019-12-31, revised 2020-03-20, initially accepted for publication 2020-04-07, published in October 2020

damages and analysis of the mechanical vibration signals. This fact results from considerable changes of the signal because of the occurrence of the damage, and thus the ease of analysis. The deep learning methods have also been used to distinguish between most important motor damages: broken rotor bar, bearing damage, inter-turn short circuit [16] and additionally unbalanced and bowed rotor [17]. However, the type of the electrical damage in [16] is not defined precisely. In [17] only one fault with three shorted turns is analysed.

Among the applied deep learning neural structures, the detection systems are mostly based on the convolutional neural networks (CNN) [14, 16, 18, 20–22] and auto-encoders [15, 19]. As shown in [14, 20], convolutional neural networks allow direct analysis of the diagnostic signal without well-known analytical methods. Moreover, CNNs are characterized by higher efficiency of the detection and evaluation of damage degree in comparison to the classical neural structures, presented in [16, 22]. Due to the principle of the CNN operation, it is necessary to adjust the input matrix accordingly. In most applications, the input signal is formed as a two-dimensional [18, 21, 22] or a three-dimensional matrix [15]. The size of the input matrix [21], the applied DNN structure [15] as well as the type of diagnostic information are directly connected with the effectiveness of the DNN-based neuronal fault detector.

All above mentioned papers deal with the detection of mechanical damages or classification between different types of motor failures. On the contrary, the main task of the diagnostic system presented in this paper is detecting the fault as well as an assessment of the IM faulty phase and stator windings damage level. The system uses the convolutional neural networks in the process of detecting inter-turn short-circuits. Diagnostic information contained in signals coming from the direct field-oriented control (DFOC) structure was used in research.

The paper is divided into 6 numbered sections. Next one presents shortly the applied control system of the induction motor drive. Then, the experimental setup is shown. The following section shows the transients of state variables and inner signals from the field-oriented control structure. Next, basics of deep neural networks, a method of generating their input vector and applied network structure are described. Successively, the training process of the network is presented, and the obtained results are analysed. Finally, the paper is shortly summarized.

2. Field-oriented control of induction motor

In this paper, the diagnostics of the stator winding damages of induction motor operating under the Direct Field-Oriented Control (DFOC) is taken in consideration. The structure of the control is shown in Fig. 1. The control system consists of four PI-type regulators: speed regulator $R\omega_m$, rotor flux amplitude regulator $R\psi_r$ and two inner regulators of stator current vector components Ri_{sx}, Ri_{sy}.

Primary speed and flux regulators define the reference values of current vector components i_{sx}^{ref}, i_{sy}^{ref}. The secondary current controllers define the reference values of stator voltage vector components u_{sx}^{ref}, u_{sy}^{ref}, which, after the conversion to the stationary reference frame α–β, become the inputs of the Space Vector Modulation (SVM) block. The modulator calculates the duty cycles k_A, k_B, k_C of the Voltage Source Inverter (VSI) which is supplied with a constant DC voltage u_d.

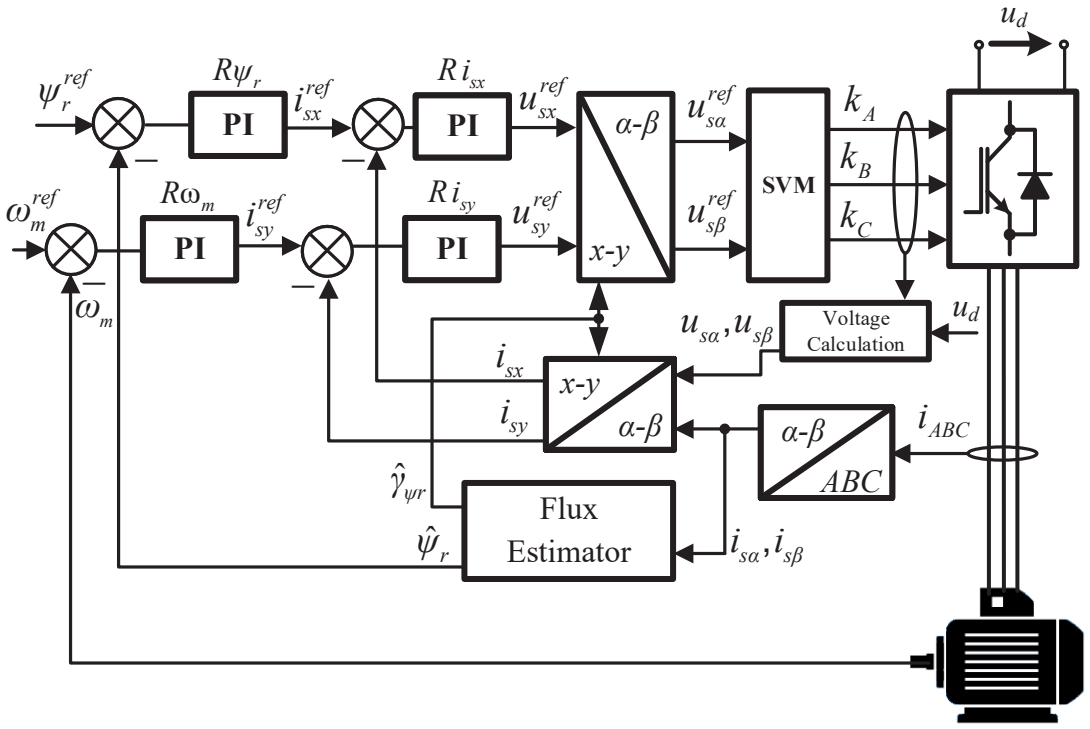

Fig. 1. Block diagram of applied field-oriented control structure

The control structure requires measurement of three phase currents i_{ABC}, the supply voltage of the inverter u_d and the motor speed ω_m. Stator voltage vector components $u_{s\alpha}$, $u_{s\beta}$ are calculated using the duty cycles and the DC-bus voltage.

To make the transformations between the stationary α–β and synchronous x–y coordinate frames possible, the knowledge about the rotor flux vector angle $\gamma_{\psi r}$ is necessary. The angle and the rotor flux amplitude ψ_r are both estimated by a rotor flux estimator (estimated values are marked with "^" symbol).

All variables in the paper are written using per-unit system, which is marked "pu" in all figures.

3. Experimental setup

Experimental tests have been conducted using the setup, shown in Fig. 2. This setup consists of two motors, the tested 3 kW induction motor and 4.7 kW Permanent Magnet Synchronous Motor (PMSM), generating the load torque. Both motors are supplied with classical two-level industrial frequency converters. The converters operate with switching frequencies of 10 kHz (IM) and 8 kHz (PMSM), respectively. The control signals for the first converter IGBTs are transferred with fibre optics. The hardware based dead time of 2 µs is ensured by a specially designed electronic system.

Three phase currents, DC-bus voltage and rotational speed are measured, using LEM transducers and incremental encoder, respectively. The impulses of the encoder are counted by the FPGA NI PXI-7851R, part of the rapid prototyping unit by National Instruments (NI).

The whole setup is controlled and coordinated by real time controller NI PXIe-8840. It defines the control signals, based on measurements, and sets required load torque value. Visualization and data acquisition process is made with usage of the VeriStand software. The neural network training and testing have been done offline using MATLAB software. During experimental verification (online research) the proposed diagnostic procedure is implemented using LabView.

4. Test results for continuous operation

Figure 3 shows exemplary transients of selected signals obtained during the start-up, constant speed operation $\omega_m = 0{,}5$ and load torque changes, from zero $m_o = 0$ to nominal value $m_o = m_n$:

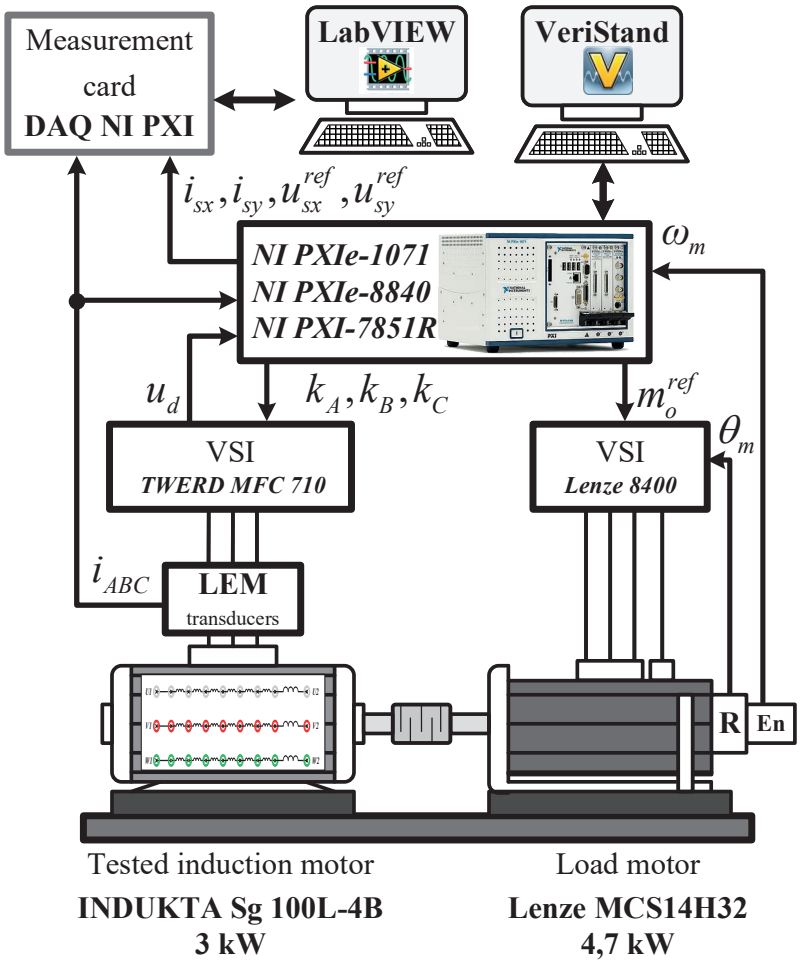

Fig. 2. Block diagram of the experimental setup

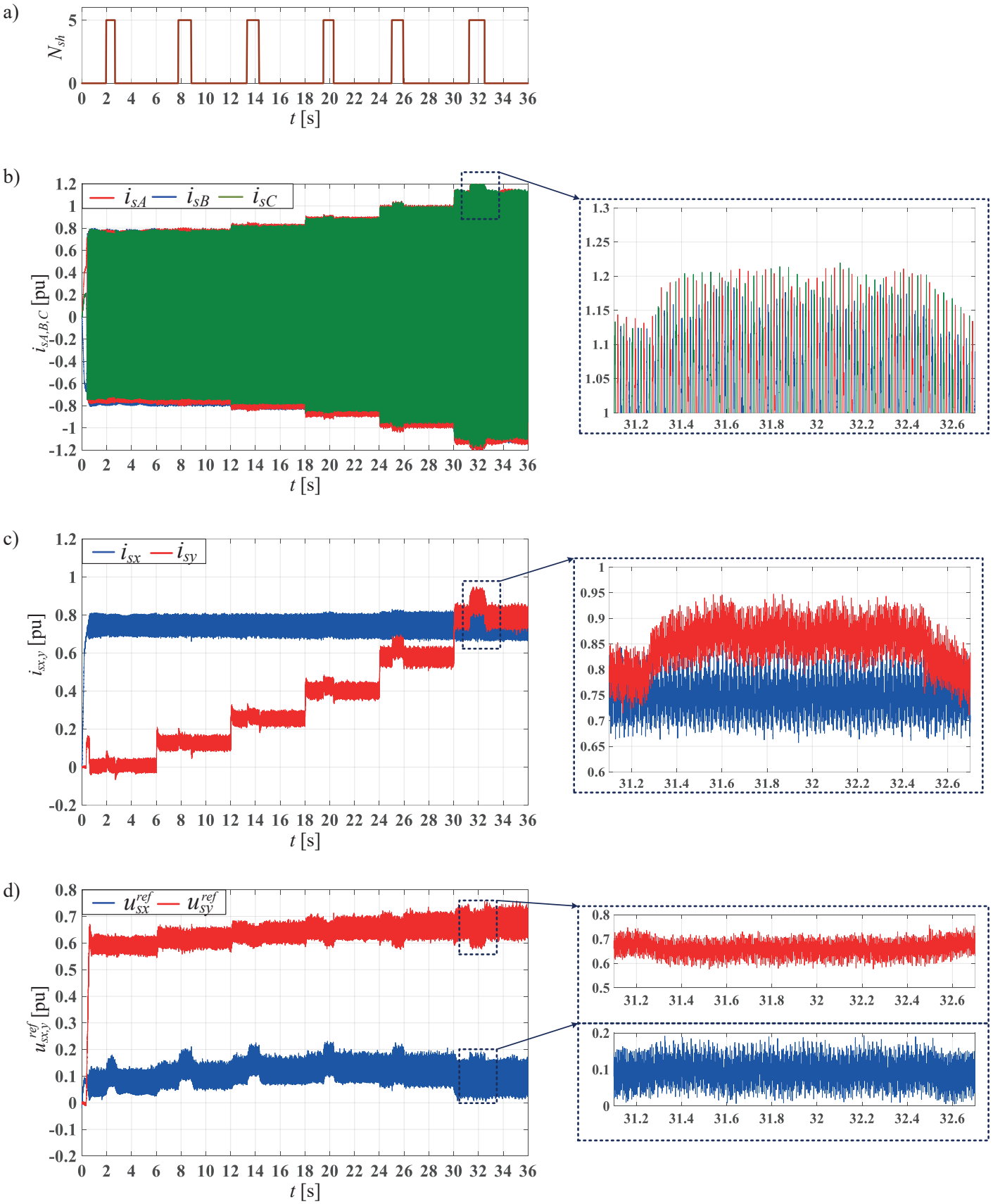

Fig. 3. Transients of selected signals during start-up, constant speed operation $\omega_m = 0.5$ and stepwise varying load torque $m_o = 0{:}m_n$ under temporary shortage of five shorted turns $N_{sh} = 5$ in phace C: a) number of shorted turns, b) phase currents, c) stator current components in synchronous reference frame, d) stator vector components in synchronous reference frame

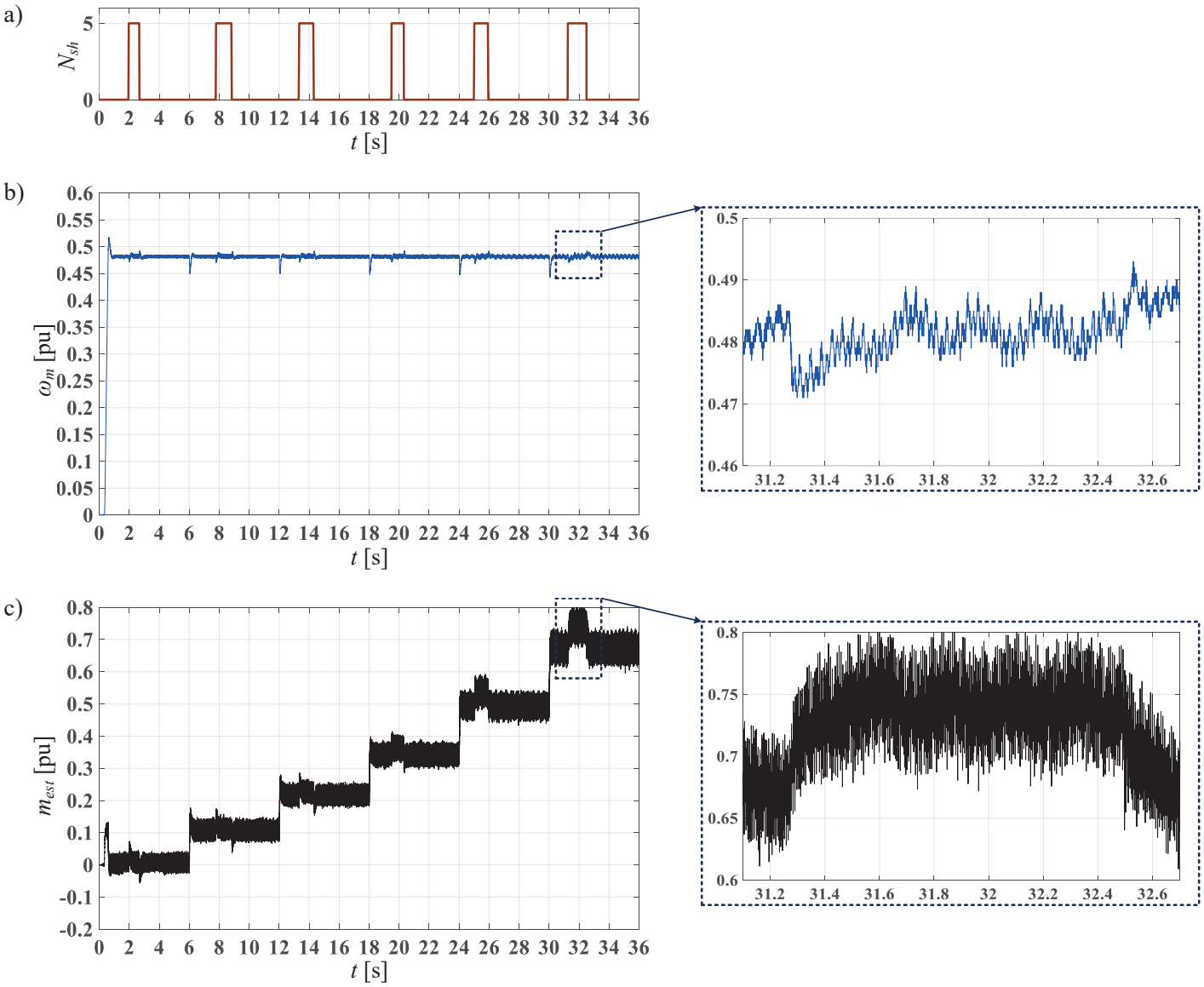

Fig. 4. Transients of selected signals during start-up, constant speed operation $\omega_m = 0{,}5$ and stepwise varying load torque $m_o = 0{:}m_n$ under temporary shortage of five shorted turns $N_{sh} = 5$ in phase C: a) number of shorted turns, b) motor speed, c) estimated electromagnetic torque

(b) motor phase currents; signals from the control structure: components of stator current (c) and voltage (d) vectors in synchronous reference frame. Figure 4 shows motor speed (b) and estimated electromagnetic torque (c).

After each change of the load torque, a metallic short-circuit of 5 turns has been modelled, each one for about 1–2 seconds (as shown in Fig. 3a). It can be seen that the short-circuit of several turns in one coil causes a momentary, non-significant change of i_{sx} current component and both u_{sx} and u_{sy} reference voltage components. Only the value of the i_{sy} component varies significantly and permanently after the damage occurrence. Due to the field orientation of the control structure, the shape of the electromagnetic torque (Fig. 4c) is analogous to the y-axis current vector component (Fig. 3c), as the rotor flux amplitude is stabilized. Speed of the motor (Fig. 4b) is almost constant during the operation, then decreases slightly after a sudden change of the load torque appears and then returns to the reference value immediately. Slightly larger oscillations of the speed can be observed during the fault occurrence comparing to the non-faulty operation as well.

Moreover, some additional oscillations can be seen in internal signals of the control structure. According to [23], it can be stated that this relates to the appearance of an additional $2f_s$ frequency harmonic (f_s is the supply frequency). The influence of the load torque on the signal values is negligible. It is worth to notice, that there is no necessity to determine the actual value of the supply frequency in the case of the proposed DNN.

Values of the stator phase current amplitudes practically do not react to the damage. This kind of failure does not cause the reaction of industrial overcurrent protections in its initial stage. However, it spreads to consecutive turns (coils) very fast, therefore fast diagnostic system is necessary.

5. Deep learning neural networks

The use of deep learning methods in the electric machine damage detection systems is currently a novelty in the field of diagnostics systems. Deep neural networks allow to depart from the principles of developing structures resulting from the theorem of universal approximation. A distinctive feature of deep learning neural structures is the use of an increased number of hidden layers as well as an increase in network learning levels. Therefore, the goal of deep learning is both to acquire prediction of the output based on the input information as well as to understand the basic features of the input matrix. One of the groups of deep neural networks are convolution neural networks (CNN). A distinctive feature of the CNN is the extraction of higher order features from signals using the convolution operation. The use of CNN in the signal analysis allows the detection of the basic signal features as well as interactions between them. Depending on the task of CNN, structures containing many convolutional segments can be used.

The use of deep learning methods in diagnostic tasks forces appropriate memory match, computational capabilities, as well as selecting the developed structure depending on the function. Nevertheless, the current state of development of microprocessor technology enables the implementation of DNN in microcontroller systems. The practical implementation of DNN was presented, among others, in [24, 25], where the authors show the possibility of implementing DNN in microcontrollers from the ARM Cortex M3 [24] and ARM Cortex-A9 [25] families.

As demonstrated in [24, 25] the use of microcontrollers based on RISC (Reduced Instruction Set Computing) architecture allows to achieve high performance of applications based on deep learning methods. In conclusion, deep learning methods are currently not a problem from the hardware implementation point of view. There are many hardware solutions containing deep network libraries [26]. Consequently, it is possible to develop and later perform the detection and classification systems based on the available microcontrollers.

5.1. Development the input matrix of the convolutional neural network. The principle of CNN operation forces the appropriate adaptation of network input matrices. Figure 5 presents the method of processing diagnostic signals into a CNN input packets. To detect machine defects, the research used the data coming from the control structure. The learning and testing samples were developed in three steps:

1) Measurement of 2000 samples of selected diagnostic signals $\left(i_{sx}, i_{sy}, u_{sx}^{ref}, u_{sy}^{ref}\right)$ which constituted the elements of vector.
2) Conversion of the vector into 40×50 matrices.
3) Recording of selected matrices containing diagnostic signal samples into 2D and 3D matrices.

The use of 2000 samples of individual diagnostic signals enabled the measurement time to be reduced to 0.2 seconds. Analytical diagnostic methods using e.g. FFT (Fast Fourier Transform) analysis require a much longer measurement time, reaching several seconds while ensuring stationary measurement (constant speed, load torque, etc.). In practical applications, ensuring the stationarity cannot be achieved in most cases. Therefore, the limitation of the measurement time resulting from the direct analysis of the diagnostic signal by the neural network is an undoubted advantage.

During experimental research, the impact of the information contained in the input vector on the effectiveness of detection and classification of IM faults by the neural network was analysed.

5.2. The structure of convolutional neural network. The basic function of the convolutional networks is to extract the features of higher orders using the operation of mathematical convolution. These networks do not have a predetermined architecture, parameters of training process or rules regarding the number of convolution layers. The CNN structure should be seen as progressing with each additional convolutional layer, allowing to extract more features of the input matrix. Therefore, the network structure depends on the type of information provided, as well as the function performed by CNN. Figure 6 presents the diagram of the proposed CNN structure, which performs the task of recognizing the degree of IM stator damages. Because of the direct use of the diagnostic signal, the developed structure contains 5 convolution sets. These sets, marked with a blue envelope in Fig. 6, act as feature detectors. The other

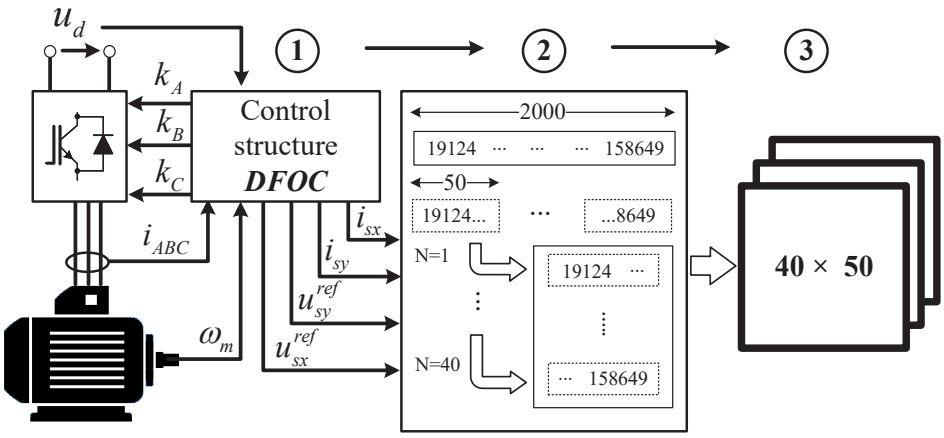

Fig. 5. Elaboration of the input layer of the CNN– schematic diagram

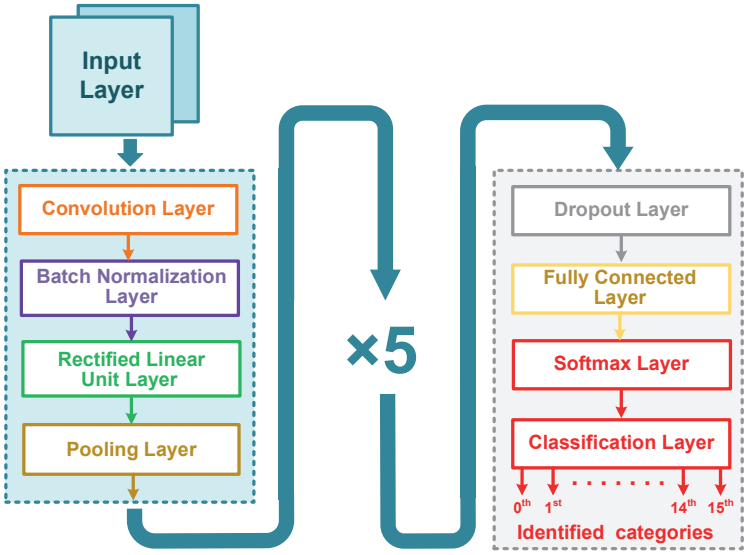

Fig. 6. Schematic diagram of the developed structure of the convolutional neural network

parts of the CNN structure allow to assign an input vector to one of the initially predefined categories. At the initial stage of the research, many different CNN structures have been analysed. The structure presented in Fig. 6 is characterized by the highest level of the effectiveness for 2 different data packets.

The basic structure of the CNN shown in Fig. 6 includes the following layers:

- convolution layers,
- batch normalization layers,
- activation layers (in the paper, the Rectified Linear Unit layer – ReLU function is used),
- pooling layers.

Their task is to determine the characteristic features of the input matrix CNN for assignment to one of the specific categories. The principle of the operation of the CNN layers is discussed inter alia in [27, 28]. The main task of the last members of the CNN structure is the assessment of belonging to one of the categories on the basis of the information about the characteristic features of the input matrix. For this purpose, the following layers are used:

- dropout layer,
- fully connected layer,
- softmax layer,
- classification layer.

In addition, these layers are provided to reduce the time of the training process as well as to prevent over-fitting.

5.3. The process of training the CNN. The training process of deep neural networks is usually carried out with gradient descent algorithms. During the study, a Stochastic Gradient Descent with Momentum (SGDM) algorithm was used. SGDM algorithm is characterized by following the gradient of randomly selected mini batch of training data. To accelerate the learning process, in the SGDM method, the step value is calculated based on the information about subsequent value of the gradients.

The size of the step depends on how many successive gradients indicate the same direction. The SGDM is an iterative algorithm, which means that it requires the initial values from which the first iteration begins. The effectiveness of the training process is strongly dependent on the initial learning rate used during the training process. At present, correct methods for selecting the initial values are not specified. In most cases, the hyperparameter values are selected empirically based on the analysis of the learning curves. Table 1 presents the hyperparameters of the applied layers of the CNN, while Table 2 shows the parameters of the training process.

Table 1
Hyperparameter of CNN layers

Hyperparameter of NN	Value of hyperparameter
Number of convolutional layers	5
Number of filters	30–40–60–80–100
Filter size	5×5
Padding / size	"*same*" / (3×3)
Number of pooling layers	5
Pooling method	*Maximum*
Pool size	5×5
Padding / size	"*same*" / (4×4)
Number of activation layers	5
Type of activation functions	*ReLU*
Number of normalization layers	5
Value of "ε" factor	0.0001
Number of dropout layers	1
Probability	0.5
Number of fully connected layers	1
Number of neurons	16

Table 2
Parameters of CNN training process

Parameter of CNN	Value of CNN Training Parameter	
Learning method	Stochastic Gradient Descent with Momentum	
Applied training data packet	i_{sx}, i_{sy}	u_{sx}^{ref}, u_{sy}^{ref}
Momentum coefficient	0.95	0.95
Initial learning rate	0.008	0.012
Number of training epochs	1000	1000
Training rate dropping method	"*piecewise*"	"*piecewise*"
Drop period	30	30
Training matrix size	40×50×2×4000	40×50×2×4000
Testing matrix size	40×50×2×4000	40×50×2×4000
Validation frequency	32	32
Shuffle method	"*every-epoch*"	"*every-epoch*"
Mini batch size	128	128
Number of categories N_c	16	16

Sixteen categories have been defined: one healthy state and fifteen unhealthy states – five different numbers of shorted turns ($N_{sh} = 1, 2, 3, 4, 5$) for each of three motor phases. The categories are defined in Table 3 in detail.

Table 3
Experimental verification of CNN structure

Phase	Number of shorted turns N_{sh}					
	0	**1**	**2**	**3**	**4**	**5**
A	0	1	2	3	4	5
B	0	6	7	8	9	10
C	0	11	12	13	14	15

5.4. Operation of the proposed CNN. The proposed CNN has been trained using the rules presented in previous section and applied to the data collected in Fig. 3. The obtained results are shown in Fig. 7 and Fig. 8, for no-load and nominal load torque operation, respectively. The figures show the analysis of

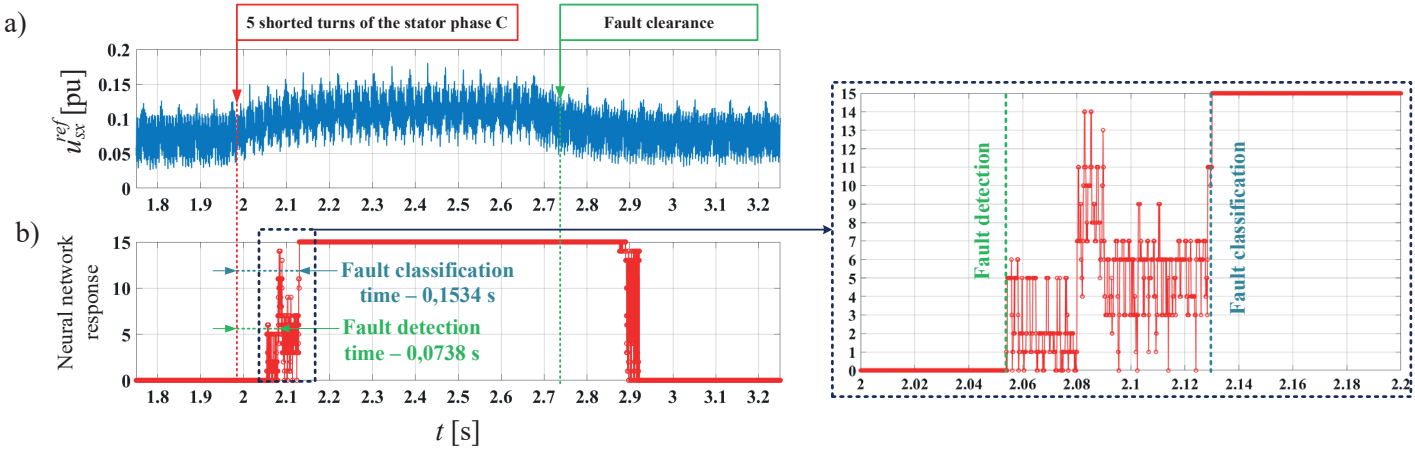

Fig. 7. CNN response during no-load motor operation: a) reference x-axis voltage vector component (part of Fig. 3d), b) response of the CNN (output category of the damage)

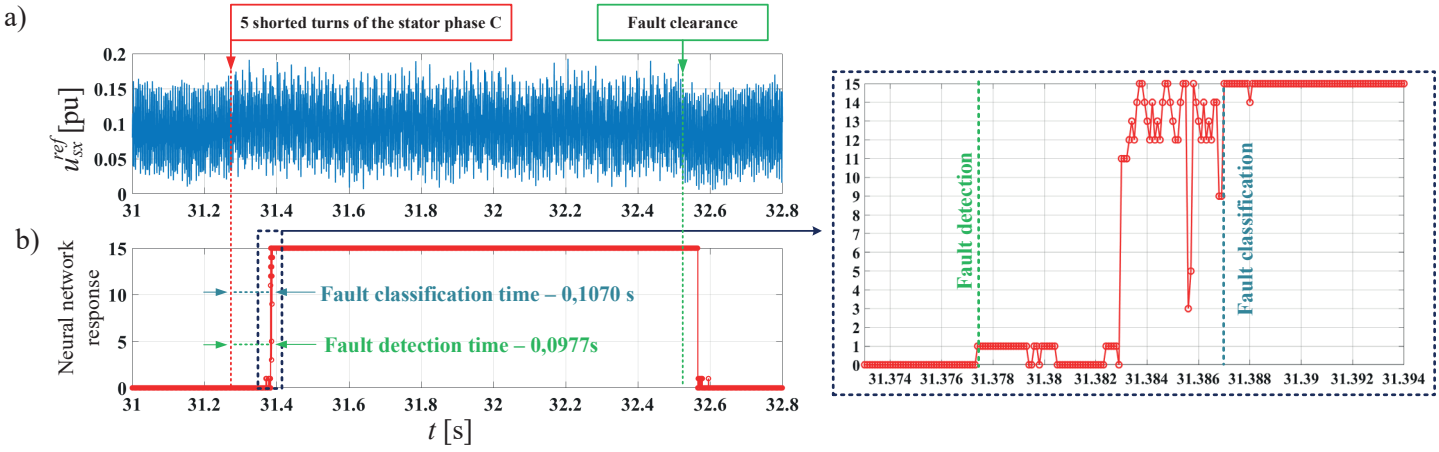

Fig. 8. CNN response during nominal load motor operation: a) reference x-axis voltage vector component (part of Fig. 3d), b) response of the CNN (output category of the damage)

one of four signals taken into consideration, i.e. x-axis voltage vector component. Two different stages of the network operation can be distinguished: first one – the temporary one, after the fault is detected for the first time and before the output is stabilized. The fact that the fault is detected is indicated by the first appearance of an output category that is different than 0. The fault is marked as classified when the obtained category value stays unchanged in subsequent steps.

As can be seen the classification time of the network is very small. However, it depends on the value of the torque. It is significantly longer in the case of the no-load operation than in the case of nominal load torque. In both presented cases the detection and the classification of the damage is correct, because five turns are shorted in phase C (category number 15 – Table 3).

5.5. Analysis of the effectiveness of the CNN structure. The process of experimental verification of the developed CNN structure was analysed in terms of the diagnostic signal that carried information about the technical condition of the tested machine. For this purpose, test data packets were transferred to the CNN input layer. The assessment of the effectiveness of structures was divided into two categories: detection efficiency and effectiveness of the stator damages degree classification. Detection efficiency η_D is the ability of the CNN network to distinguish correctly between symptoms of the damaged and undamaged motor. The classification efficiency η_C combines both detection and distinction of the degree of stator damage (faulty phase and number of shorted turns). The results of experimental tests for the 2 sets of the diagnostic signals presented in Table 4 were calculated in accordance with the following equations:

$$\eta_D = \frac{X_P}{X_F + X_U}, \tag{1}$$

$$\eta_C = \frac{1}{N_C} \sum_{i=1}^{N_C} \frac{X_{Pi}}{X_i}, \tag{2}$$

where:
X_P – the number of positive (correct) neural network responses,
X_F – number of induction motor faulty states,
X_U – number of induction motor unfaulty states,
$N_C = 16$ – number of considered categories,
$X_{P0–15}$ – the number of positive (correct) neural network responses for categories 0 to 15,
$X_{0–15}$ – number of considered cases in each category.

Table 4
Experimental verification of CNN structure

Parameter	**Value of Parameter**	
Applied testing data packet	i_{sx}, i_{sy}	u_{sx}^{ref}, u_{sy}^{ref}
Stator winding faults detection effectiveness (η_D)	98.9%	98.2%
Stator winding fault classification effectiveness (η_C)	91.3%	89.7%

The analysis of the experimental verification results allowed to state that the detection efficiency was over 98% in the case of diagnostic signals coming from the control structure. It is worth noting that the same structure was used for the 2 discussed CNN testing data packets (current vector components, reference voltage vector components) and almost the same detection results have been obtained. Accordingly, it can be concluded that the features of the damage in the diagnostic signals are reflected in a similar way, so they are features of the same order. As observed during experimental verification, the damage classification efficiency index was smaller than the detection efficiency index. This fact results from small quantitative changes in diagnostic signals due to a short circuit in various phases of the stator windings. In addition, it should be noted that during the measurements, 2000 signal samples were taken each time, regardless of the frequency of the supply voltage. Therefore, the developed matrices of input signals may be subject to some shifts between successive samples. Nevertheless, the developed structure was not dependent on the load torque as well as frequency of the supply voltage.

6. Conclusions

Presented convolutional neural network is characterized by a high efficiency in the detection of IM electrical faults. The detector based on the CNN constitute ensures high level of both damage and classification efficiencies. The damage was detected in around 98% cases and most of the detection errors have been made in the case of one shorted turn. The network is also able to distinguish shorted phase and number of shorted turns in stator winding with about 90% of effectiveness. Thus, the developed detection system is less effective in the task of assessment the degree of damage. However, it should be pointed out that the main task of diagnostic systems is to detect damage at an early possible stage. Further assessment of the level of damage constitutes a secondary goal of diagnostic applications.

Moreover, the advantage of the proposed CNN-based fault detector is its very short diagnostic time. By using direct signal analysis, it was possible to limit the detection process time to maximum 0.2 seconds, which is an undoubted advantage due to the nature of the discussed damages. The advantage of the presented CNN application is also the use of signals from the control system without the need for additional measuring systems. The knowledge about the frequency of diagnostic signals is not necessary as well. Therefore, the presented solution may be an alternative to motor fault detectors based on classical neural networks in the future.

Acknowledgements. This research was supported by the National Science Centre (Poland) under grant number 2017/27/B/ST7/00816.

References

[1] W.T. Thomson and M. Fenger, “Current signature analysis to detect induction motor faults”, *IEEE Ind. Appl. Mag.* 7, 26–34 (2001).

[2] C.T. Kowalski, "Diagnostics of drive systems with an induction motor using artificial intelligence methods", *Oficyna Wydawnicza Politechniki Wrocławskiej*, Wrocław, Poland, (2013) [in Polish].

[3] N. Bessous, S. Sbaa, and A.C. Megherbi, "Mechanical fault detection in rotating electrical machines using MCSA-FFT and MCSA-DWT techniques", *Bull. Pol. Ac.: Tech*. 67(3), 571–582 (2019).

[4] F. Wilczyński, P. Strankowski , J. Guziński , M. Morawiec, and A. Lewicki, "Sensorless field oriented control for five-phase induction motors with third harmonic injection and fault insensitive feature", *Bull. Pol. Ac.: Tech*. 67(2), 243–262 (2019).

[5] S.M.A. Cruz and A.J.M. Cardoso, "Stator winding fault diagnosis in three-phase synchronous and asynchronous motors, by the extended Park's vector approach", *IEEE Trans. Ind. Appl.* 37, 1227–1233 (2001).

[6] M. Wolkiewicz and C.T. Kowalski, "Incipient stator fault detector based on neural networks and symmetrical components analysis for induction motor drives", in *13th Selected Issues of Electrical Engineering and Electronics (WZEE)*, Rzeszów, Polnad, 1–7 (2016).

[7] M. Skowron, M. Wolkiewicz, T. Orlowska-Kowalska, and C.T. Kowalski, "Effectiveness of Selected Neural Network Structures Based on Axial Flux Analysis in Stator and Rotor Winding Incipient Fault Detection of Inverter-fed Induction Motors", *Energies* 12, 2392, 1–20 (2019).

[8] V.N. Ghate and S.V. Dudul, "Optimal MLP neural network classifier for fault detection of three phase induction motor", *Expert Syst. Appl.* 37(4), 3468–3481 (2010).

[9] C.T. Kowalski and M. Wolkiewicz, "Stator faults of the converter-fed induction motor using symmetrical components and neural network", in *13th European Conf. on Power Electronics and Appl. (EPE)*, Barcelona, Spain, 1–6 (2009).

[10] C.T. Kowalski and M. Kamiński, "Rotor fault detector of the converter-fed induction motor based on RBF neural network", *Bull. Pol. Ac.: Tech.* 62(1), 69–76 (2014).

[11] M. Skowron, M. Wolkiewicz, T. Orlowska-Kowalska, and C.T. Kowalski, "Application of Self-Organizing Neural Networks to Electrical Fault Classification in Induction Motors", *Appl. Sci.* 9(4), 616 (2019).

[12] O. Sid, M. Menaa, S. Hamdani, O. Touhami, and R. Ibtiouen, "Self-organizing map approach for classification of electricals rotor faults in induction motors", in *2nd Int. Conf. on Electric Power and Energy Conversion Systems (EPECS)*, Sharjah, United Arab Emirates, 1–6 (2011).

[13] X.L. Ying and W.N. Lan, "Motor Fault Diagnosis Based on Wavelet Neural Network", in *2nd Int. Conf. on Intelligent Computation Technology and Automation*, Changsha, Hunan, China, 553–555 (2009).

[14] G. Xu, M. Liu, Z. Jiang, W. Shen, and C. Huang, "Online Fault Diagnosis Method Based on Transfer Convolutional Neural Networks", *IEEE Trans. Instrum. Meas.* 69(2), 509–520 (2019).

[15] E. Principi, D. Rossetti, S. Squartini, and F. Piazza, "Unsupervised electric motor fault detection by using deep autoencoders", *IEEE-CAA J. Automatica Sin.* 6(2), 441–451 (2019).

[16] P. Chattopadhyay, N. Saha, C. Delpha, and J. Sil, "Deep Learning in Fault Diagnosis of Induction Motor Drives", in *Prognostics and System Health Management Conference (PHM-Chongqing)*, Chongqing, 1068–1073 (2018).

[17] S. Shao, S. McAleer, R. Yan, and P. Baldi, "Highly Accurate Machine Fault Diagnosis Using Deep Transfer Learning", *IEEE Trans. Ind. Inform.* 15(4), 2446–2455 (2019).

[18] X. Ding and Q. He, "Energy-fluctuated multiscale feature learning with deep convnet for intelligent spindle bearing fault diagnosis", *IEEE Trans. Instrum. Meas.* 66(8), 1926–1935 (2017).

[19] T. Junbo, L. Weining, A. Juneng, and W. Xueqian, "Fault diagnosis method study in roller bearing based on wavelet transform and stacked auto-encoder", in *IEEE 27th Control Decis. Conf.*, Qingdao, China, 4608–4613 (2015).

[20] S. Afrasiabi, M. Afrasiabi, B. Parang, and M. Mohammadi, "Real-Time Bearing Fault Diagnosis of Induction Motors with Accelerated Deep Learning Approach", in *10th Int. Power Electronics*, *Drive Systems and Technologies Conf. (PEDSTC)*, Shiraz, Iran, 155–159 (2019).

[21] L. Wen, X. Li, L. Gao, and Y. Zhang, "A new convolutional neural network-based data-driven fault diagnosis method", *IEEE Trans. Ind. Electron.* 65(7), 5990–5998 (2018).

[22] T. Ince, S. Kiranyaz, L. Eren, M. Askar, and M. Gabbouj, "Real-time motor fault detection by 1-D convolutional neural networks", *IEEE Trans. Ind. Electron.* 63(11), 7067–7075 (2016).

[23] M. Wolkiewicz, G. Tarchała, C.T. Kowalski, and T. Orłowska-Kowalska, "Stator faults monitoring and detection in vector controlled induction motor drives-comparative study", *Advanced Control of Electrical Drives and Power Electronic Converters. Studies in Systems*, *Decision and Control*, vol. 75, pp. 169–191, ed. Jacek Kabziński, Springer, 2017.

[24] B. Karg and S. Lucia, "Deep learning-based embedded mixed-integer model predictive control," in *Proc. 2018 European Control Conf.*, Limassol, 2075–2080 (2018).

[25] J. Jin, V. Gokhale, A. Dundar, B. Krishnamurthy, B. Martini, and E. Culurciello, "An efficient implementation of deep convolutional neural networks on a mobile coprocessor," in *Proc. 2014 IEEE 57th Int. Midwest Symp. on Circuits and Systems*, College Station, USA, 133–136 (2014).

[26] STMicroelectronics, *Artificial Intelligence (AI) software expansion for STM32Cube*, STMicroelectronics Data Brief, 2019.

[27] A. Krizhevsky, I. Sutskever, and G. Hinton, "ImageNet classification with deep convolutional neural networks", *Advances in Neural Information Processing Systems*, 25, 1106–1114 (2012).

[28] S. Ioffe and C. Szegedy, "Batch normalization: Accelerating deep network training by reducing internal covariate shift", arXiv:1502.03167, (2015).